Petrology, Vol. 3, No. 6, 1995, pp. 576 - 587. Translated from Petrologiya, Vol. 3, No. 6, 1995, pp. 631 - 644.

Retrograde Vesiculation of Basic Magma in Shallow Chambers: Model of Genesis of Mafic Inclusions in Silicic and Intermediate Rocks

I. N. Bindeman

Department of Geophysical Sciences, University of Chicago, 5734 S. Ellis Ave., Chicago, IL, 60637 USA

Received February 1, 1995

Abstract – This work is devoted to a physical mechanism of the mixing of basic and silicic (intermediate) magmas contrasting in composition, temperature, density, and viscosity. The purpose is to combine natural evidence and numerical model, taking into account the influence of the vesiculation of basic magma on its density decrease, which is favorable for magma mixing. This approach is based on the fact that many silicic and basic magmas can coexist in one magma chamber for a long period of time (from years to hundreds of years). A small portion of hot basic magma, replenishing the silicic magma chamber, locates at the base of the chamber. This leads to the formation of two independently convecting sheets. As it follows from the recent fluid mechanic models of the crystallization of a sheet cooled from above, the upper part of the sheet of hot and dense basic magma crystallizes at the boundary of the cool silicic magma sheet. The crystallization front moves downward, and a layer of crystals and residual melt (mushy zone) forms. In the present work, we consider the formation of gas bubbles (retrograde vesiculation) in this crystallization layer as a result of fluid saturation during the crystallization of water-free minerals. In some cases, the three-phase mixture of gas, crystals, and residual melt becomes less dense than the overlying silicic magma. The difference in density gives rise to the formation of diapirs, which can leave the crystallization layer and intrude into silicic magma. We consider the vesicular mafic inclusions in silicic and intermediate rocks to be the result of the disruption of such diapirs. In this paper we present some natural evidence for a mechanism of inclusion formation, classify various conditions of vesiculation of basic magma under the silicic magma, and discuss a numerical model of crystallization of a density unstable layer. The proposed model is based on the solution of conservation of heat and mass equations. It is applied to the density, size, and differentiation degree of mafic inclusions in the silicic and intermediate volcanics of the Kurile Islands and Kamchatka.

INTRODUCTION

Petrological observations of plutonic and volcanic rocks show that, in some cases, basic and silicic magmas apparently coexisted throughout the lifetime of the magma chamber (Wiebe, 1993; Freundt and Schmincke, 1992; Litvinovskii *et al.*, 1992). The intruded dense basic magma forms an independent hot sheet at the bottom of the chamber of cooler and less dense intermediate or silicic magma. In many cases the magma mixing is not complete, and silicic or intermediate rocks contain porous mafic inclusions (not to be confused with glomeroporphyritic cognate inclusions), which are spread over the whole magmatic body. The genesis of these inclusions is most consistent with the supercooling of drops of hot basic magma in cool silicic magma (Anderson, 1976; Sparks *et al.*, 1977; Eichelberger, 1980; Bacon, 1986; Barbarin, 1991; Koyaguchi, 1991; Bindeman, 1993). Experiments with viscous liquids demonstrate that during the replenishment of chambers with new magma portions, only a small degree of mixing is possible between basic and silicic magmas because of the large difference in their viscosities (Campbell and Turner, 1985, 1989; Turner and Campbell, 1986). Even in the case of forced injection into the chamber, basic magma does not break up into drops, but rather, falls to the bottom of the chamber. As a result, a stable stratification develops with two magma sheets of different densities (Turner and Campbell, 1986). Inclusion formation and magma mixing now require the basic magma to overcome the density barrier.

In this paper we address the density decrease of basic magma which results from its vesiculation immediately under the silicic magma sheet.

PREVIOUS WORKS AND FORMULATION OF PROBLEM

J.C. Eichelberger (1980) found that some mafic inclusions are less dense than the host silicic rocks. The inclusions have a large porosity that plausibly inherits the vesiculation of basic magma while still in a magma chamber or conduit. In this model, the inclusions form after the sheet of partly crystallized and vesiculated basic magma becomes less dense than the overlying sheet of silicic magma. As a result, Rayleigh–Taylor instability develops, and the mafic inclusions can break

off the sheet of basic magma and penetrate into the interior of the silicic magma chamber.

H.E. Huppert *et al.* (1982) and Thomas *et al.* (1993) reproduced mixing and inclusion formation in experiments on liquids with different initial densities by gas release in the lower, denser liquid. However, these authors considered only an isothermal case, when the whole sheet of basic magma underwent vesiculation. In nature, we should expect preferential crystallization of basic magma from above upon contact with the silicic magma due to the higher temperature gradient.

A two-phase (melt + crystals) layer forms at the upper boundary of a liquid sheet under cooling from above in crystallization experiments (Marsh, 1989; Worster *et al.*, 1990). This partly crystalline layer grows downward. In frames of the two-sheet model (basic – silicic magmas), the formation of the crystallization layer results in the isolation of basic and silicic magmas and the termination of magma mixing. It seems logical that any model of the influence of gas release on mixing should presume the existence of this crystallization layer (vesiculated or not).

Three possible cases of interaction of basic and silicic sheets can be proposed (Fig. 1):

(1) no or insufficient gas bubble production in the crystallization layer, when neither density inversion nor inclusion formation occurs; (2) gas bubbles release in the crystallization layer and make it density unstable; Rayleigh–Taylor instability forms and leads to the rising of diapirs, which break off to form porous mafic inclusions; (3) gas bubbles release over the whole sheet of basic magma; this leads to bubble accumulation under the crystallization layer and to the more intense formation of diapirs; in some cases (if vesiculation is more intensive), the whole sheet of basic magma becomes density unstable and convective overturn occurs.

The first part of this paper is devoted to natural evidence of basic magma vesiculation under the silicic magma sheet. We show that the origin of inclusions in silicic and intermediate rocks of the Kurile-Kamchatka island arc may be related to this process.

In the second part, we classify possible regimes of vesiculation in the crystallization layer and discuss the different inclusion geneses.

The third part describes the results of the numerical modelling of the vesiculation processes in the crystallization layer and regimes of inclusion formation.

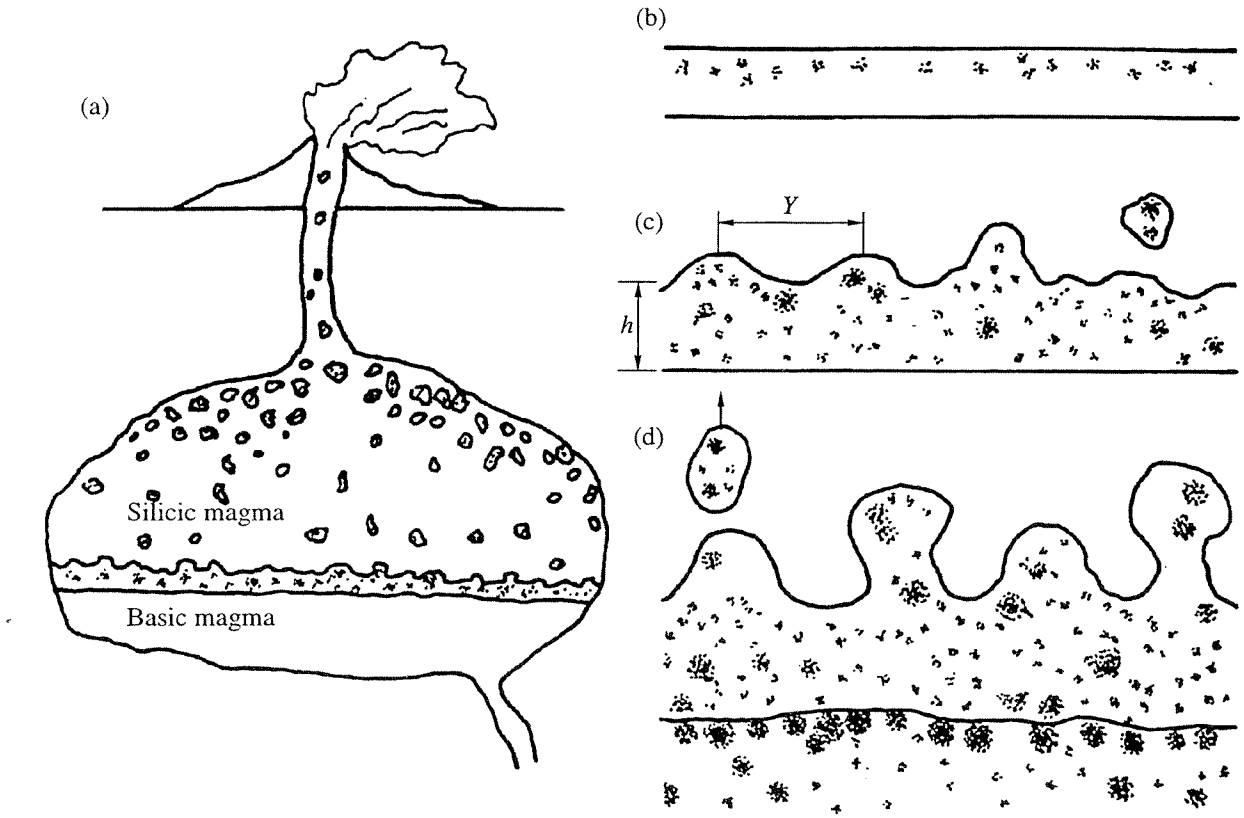

Fig. 1. Crystallization of the density unstable crystallization layer of basic magma under the silicic magma sheet and the formation of diapirs (mafic inclusions).

(a) chamber structure, (b) - (d) different paths of crystallization of the upper part of the basic magma sheet and formation of diapirs (see text). The dots show gas bubbles. Y – distance between diapir heads, h – the thickness of the crystallization layer.

NATURAL EVIDENCE OF BASIC MAGMA VESICULATION IN SHALLOW-LEVEL SILICIC MAGMA CHAMBERS

Mafic inclusions were collected and investigated in several volcanoes of the Kurile Islands and Kamchatka (Bindeman, 1991; Bindeman and Bailey, 1994; Bindeman and Podladchikov, 1991; Frolova *et al.*, 1992). Usually, they are an ellipsoidal shape and 3 - 10 cm in diameter (rarely up to 1 m). The size distribution of the inclusions is log-normal, and relatively large inclusions are more abundant (Bindeman and Podladchikov, 1991). The inclusions are composed mainly of basalts or basaltic andesites, and rarely of andesites. They consist of sparse phenocrysts in a fine-grained groundmass with volcanic glass (10 - 50% of the whole rock). Most of the inclusions show clear evidence of rapid cooling: elongated, often skeleton plagioclase microlites and fine-grained quenched rims.

Mafic inclusions from six volcanic centers in the Kurile-Kamchatka island arc are less dense than their host silicic and intermediate rocks (Table 1). Low density is always caused by the high porosity (10 - 20%) of the inclusions. It is interesting that the mafic inclusions from the six volcanoes contain amphibole microlites. Some inclusions from Japan also have amphibole in a groundmass (Koyaguchi, 1991).

To ascertain the genesis of inclusions still in a magma chamber, one must answer the question "On what depth could basic magma become less dense and buoyant?"

Figure 2 illustrates the variation in the bulk density of basic magma after 50% crystallization and the vesiculation at different depths and H_2O and CO_2 contents. For instance, at a water content of 3 - 5 wt % the basic magma may become less dense than the host silicic magma, taking into account the water dissolved in the residual melt of the basic magma. The density decrease is more pronounced for shallow (1 - 5 km) depths. This is consistent with the fact that the inclusions occur mostly on the caldera volcanoes and volcanoes with shallow magma chambers (Table 1). The presence of CO_2 in fluid enhances the effect of the bulk density decrease. This effect, however, is smaller than that of a similar mass of H_2O because of the smaller specific volume of CO_2. Increasing pressure (depth of magma chamber) decreases the effect of vesiculation on density because of gas bubble compressibility and the increase of water solubility in the residual melt of basic magma. Vesiculation may not occur at all if water dissolves completely in the residual melt. This happens at pressures above some critical value for a certain H_2O content and magma crystallinity, if hydrous fluid alone is present in the system. However, even the relatively high pressure (2 - 7 kbar) will not stop vesiculation if CO_2 is present in the fluid, as CO_2 is practically insoluble in magmas at crustal pressures (Shilobreeva and Kadik, 1985). Crystallization of 10% of the amphibole should only slightly decrease the vesiculation, as this mineral does not consume much H_2O.

The presence of amphibole in the groundmass of mafic inclusions from some volcanoes (Table 1) is solid proof of the crystallization of inclusions at certain depths and sufficiently high (2 - 4 wt %) initial water contents. Experiments on amphibole stability at different temperatures and H_2O pressures in basaltic and

Table 1. Features of mafic inclusions and host rocks in volcanoes of the Kurile-Kamchatka island arc

Volcano	Type of volcano	Depth of chamber, km	Host rock	Density of host rock, g/cm^3	Density of inclusions, g/cm^3	*n*	Presence of amphibole in groundmass of inclusions
Mendeleev (Kunashir Island);	Multicaldera stratovolcano	8	Dacite	2.39	2.16	20	–
Golovin (Kunashir Island)	Caldera	5	〃	2.33	2.25	9	–
Baranskii (Iturup Island)	Stratovolcano	2 - 3	〃	2.35	2.23	12	+
Dikii Greben' (Kamchatka)	Volcano–extrusion	No data	Rhyodacites, andesites	2.33 2.42	2.18 2.22	10 12	+ +
Kizimen (Kamchatka)	Stratovolcano	〃	Dacites	2.45	2.20	3	+
Kambal'nyi (Kamchatka)	Caldera stratovolcano	〃	〃	2.45	2.30	11	+
Shiveluch (Kamchatka)	〃	〃	Andesites	No data	No data	–	+
Bezymyannyi (Kamchatka)	Complex stratovolcano	〃	〃	〃	〃	–	+

Note: Density was measured using a hydraulic balance; *n* – number of measurements; depths of chambers are given from seismic data (Zlobin, 1989).

andesitic magmas (Eggler *et al.*, 1973; Kadik *et al.*, 1986) show that magmatic amphibole crystallizes at pressures higher than 0.5 - 1.5 kbar. Kadik *et al.* (1986) determined the amphibole stability for Kamchatka andesites by measuring the degree of crystallinity at which amphibole appeared. The aim of these experiments was to estimate the minimum water pressure and water content in magma at which amphibole begins to crystallize. For the andesites of the Klyuchevskoi Volcano, the water content in magma was in the range of 3 - 5 wt % which is typical of amphibole-bearing calc-alkaline magmas.

Thus, the inclusions, at least those with amphibole in a groundmass, apparently form from magma relatively rich in H_2O at depths greater than 1.5 - 4.5 km (0.5 - 1.5 kbar) (Eggler, 1973). Such pressures correspond to shallow-level magma chambers. However, amphibole-free inclusions need not crystallize from magma with a low H_2O content, but can form at pressures lower than 0.5 - 1.5 kbar.

If the crystallinity of basic magma increases and gas does not escape from the system, the higher water portion releases into gas bubbles and the bulk density further decreases (Huppert *et al.*, 1982). Therefore, a three-phase mixture (crystals + gas + residual melt) (Fig. 2), less dense than the host silicic or intermediate magma, forms at 50 - 70% crystallization of basic magma and a water content of 2 - 4 wt % in chambers at a depth of a few kilometers.

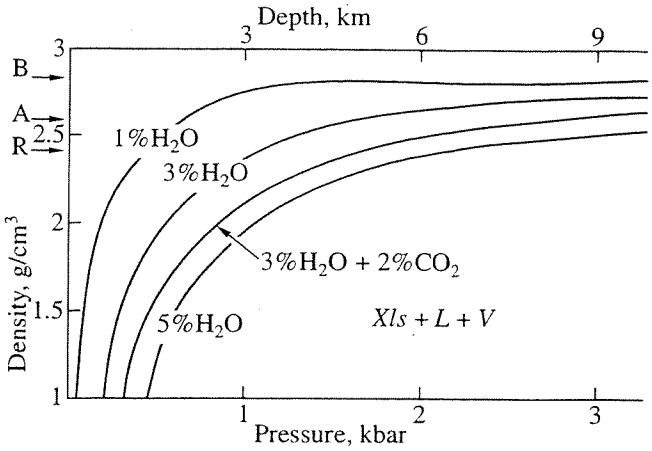

Fig. 2. Density of basic magma after 50% crystallization under the silicic magma sheet at different pressures (depths of magma chamber) and contents of water and carbon dioxide.

T = 1100°C, water solubility in basaltic magma was calculated through $N_{H_2O} = mP^n$, where m = 1.31 and n = 0.61 (Kadik *et al.*, 1973). *P–V–T* properties of H_2O and CO_2 are after Burnham *et al.* (1969) and Shmonov and Shmulovich (1978), respectively. B, A, R – "dry" densities of basalts, andesites, and rhyolites free of gas bubbles.

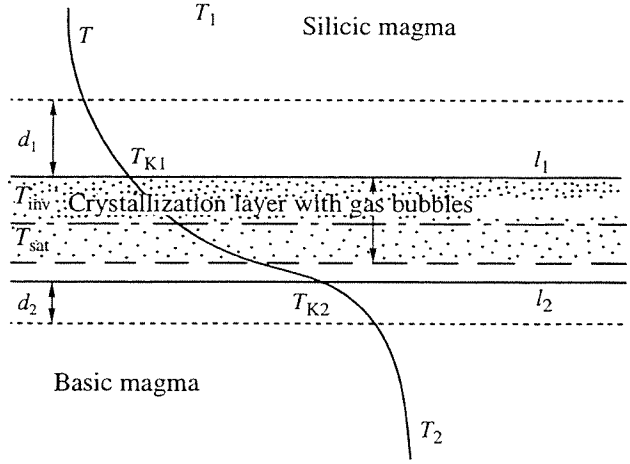

Fig. 3. Structure of a crystallization layer between basic and silicic magmas.

d_1, d_2 – thicknesses of the boundary layers; l_1, l_2 – the upper and lower boundaries of the crystallization layer; see Table 2 for other parameters.

STRUCTURE OF THE CRYSTALLIZING PART OF THE BASIC MAGMA SHEET

Consider the temperature profile through the crystallizing portion of the basic magma sheet under the silicic magma sheet (Fig. 3). Temperature drops from the hot basic magma upward to the overlying cool silicic magma and causes the formation of a crystallization layer. This layer may be divided into two zones: a rheologically rigid zone, where crystallinity is more than 50 - 60%, and a "mushy" zone, where crystallinity is 25 - 50% (Marsh, 1989). In addition to Marsh's assumptions, we suggest that gas bubbles may be present in each zone, and gas does not leave the crystallization layer until almost complete crystallization (for discussion see Huppert *et al.*, 1982). Within the rigid zone, the movement of neither gas bubbles nor crystals is possible. Within the mushy zone and below it, a limited gas bubble flotation and crystal sinking may occur. The lower boundary of the mushy zone either corresponds to the isotherm of convective liquidus (Marsh, 1989) or is a hydrodynamic boundary layer related to convection intensity in the basic magma sheet (Worster *et al.*, 1990).

The structure of the crystallization layer with gas bubbles is determined by the relative position of five isotherms shown in Fig. 3.

— two isotherms of contacts T_{K1} and T_{K2} corresponding to the upper (l_1) and the lower (l_2) boundaries of the crystallization layer (Table 2);

— isotherm T_{50} of 50% crystallinity (boundary between mushy and rigid zones);

— isotherm of gas saturation T_{sat}, above which, gas bubbles form;

— isotherm of density inversion T_{inv}, above which, the three-phase mixture of crystals, gas, and residual melt is less dense than the overlying magma sheet.

Figure 3 shows that for a horizontal and flat crystallization layer, all isotherms are parallel and serve as physical boundaries between zones with different

Table 2. Parameters and their initial values used in calculations

Parameters and units of measurement		Silicic magma	Basic magma
T	temperature, °C	T_1	T_2
T_K	temperature of contact	T_{K1}	T_{K2}
T_l	temperature of liquidus	900	1200
T_s	temperature of solidus	700	800
T_{sat}	temperature of fluid saturation		
T_{inv}	temperature of density inversion		
T_{50}	temperature of 50% degree of crystallinity		
z	vertical coordinate, m		
LL	thickness of magma sheet, m	10	1000
h	thickness of buoyant crystallization layer, m		
n	frequency of diapir production, s^{-1}		
Y	distance between diapir heads, m		
l_1	the upper boundary of crystallization layer, m		
l_2	the lower boundary of crystallization layer, m		
d	thickness of boundary layer, m	d_1	d_2
V	velocity of downward propagation of boundary l_1, cm/s		
a, b, c	parameters		
Cef	effective heat capacities, cal/g deg	$C1ef = 3.3$	$C2ef = 5.5$
Xls	crystallinity, vol %		
f	increase of degree of crystallinity at cooling by 1°C		
λ	thermal conductivity, cal/g deg	λ_1	λ_2
k	thermal diffusivity, cm^2/s	0.005	0.005
β	coefficient of thermal expansion	10^{-5}	10^{-5}
q	latent heat of crystallization, cal.	$q_1 = 300$	$q_2 = 400$
ρ	density, g/cm^3	2.4	2.65
$\Delta\rho$	density difference between silicic magma and diapirs 0.1 g/cm^3		
μ	viscosity, poise	106	103
μ_3	effective viscosity of the buoyant crystallization layer		
F	convective heat flux, cal/cm^2 s		
Ra	Rayleigh number		
J	heat fluxes, cal/cm^2	J_1	J_2
J_3	heat flux connected with diapirs		
m	mass of a diapir, g		
g	free-fall acceleration, cm/s^2		

Note: Values are from (Sharapov and Cherepanov, 1985; Huppert and Sparks, 1988).

contents of crystals and gas bubbles. The relative position of the isotherms is governed by initial fluid content, depth of magma chamber, magma composition, and some other parameters.

REGIMES OF VESICULATION

Figure 4 summarizes all possible combinations of the relative position of the isotherms, defining the possibility and regimes of vesiculation in the crystallization layer.

Regime 1a, 1b: $T_{K1} > T_{inv}$, i.e., the density inversion isotherm is located higher than the isotherm of the upper contact. Crystallization proceeds without vesiculation (1a) or with insufficient vesiculation within the rigid zone (1b). Gas motion, density inversion, and inclusion formation are impossible. The basic magma sheet will solidify under the silicic magma sheet.

Regime 1c, 1d: $T_{K1} > T_{inv}$, but $T_{sat} > T_{K1}$. Crystallization releases gas bubbles within the mushy zone (1c), or even over the entire volume of the basic magma sheet (1d) below the lower boundary T_{K2}. However, the gas

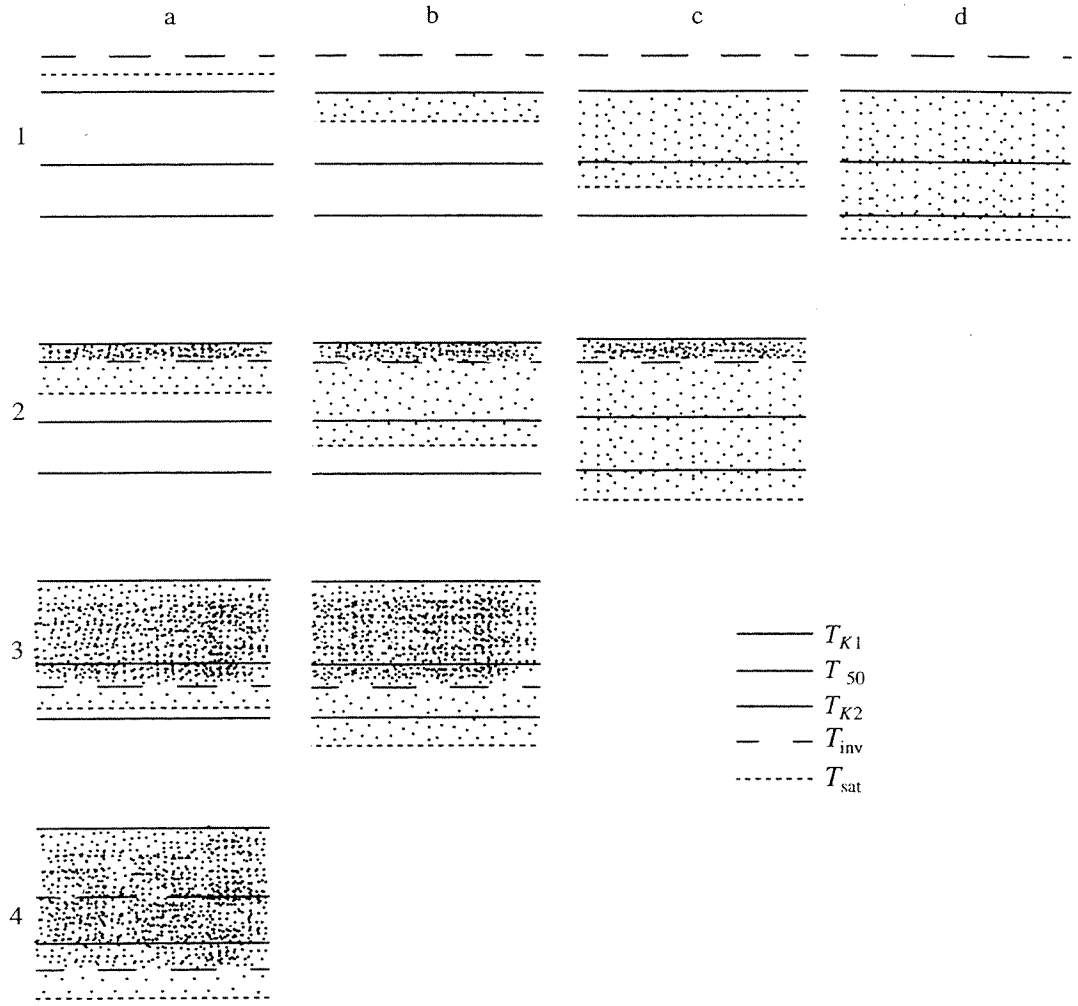

Fig. 4. Relative position of isotherms defining possible regimes of vesiculation.
The layer saturated with gas bubbles is marked with sparse dots; layer less dense than the overlying one is marked by dense dots; solid lines – isotherms T_{K1}, T_{50}, and T_{K2}, from top to bottom in each picture.

bubble content is insufficient for density inversion and inclusion formation. Nevertheless, gas bubbles can float and concentrate under the rigid zone (or the boundary between two magmas), and eventually density inversion occurs.

Regimes 2 - 4 assume that $T_{K1} < T_{inv}$. In these cases, a certain zone within the crystallization layer becomes buoyant because of extensive vesiculation, and inclusion formation is possible.

In regime 2a, a thin part within the rigid zone is density unstable, and gas bubble flotation does not occur. Regimes 2c and 2d allow gas bubble flotation up to the rigid zone and, therefore, the density difference between the rigid zone and overlying silicic magma sheet increases.

Regimes 3a and 3b assume density inversion within the rigid zone and part of the mushy zone, and these zones become buoyant. Additionally, gas bubbles rising from below should increase the density instability.

In regime 4, density inversion involves the whole crystallization layer or even the whole sheet of basic magma. In this case, density inversion can lead to the flotation of the whole vesiculated sheet of basic magma, effective mixing, and the formation of numerous porous mafic inclusions (Huppert *et al.*, 1982).

The vesiculation regimes are not stationary and invariable. With cooling, the vesiculation tends to develop from regime 1 to regime 4, as the concentration of gas bubbles increases in the crystallization layer. In other words, temperatures T_{inv} and T_{sat} are more or less fixed for a given magma at a given depth and initial fluid content, but temperatures at contacts, T_{K1} and T_{K2}, and within the magma sheet decrease during crystallization. Each regime has its peculiar dynamics of instabilities and inclusion formation.

Case 1. Crystallization of the mafic magma sheet proceeds without diapir (inclusion) formation.

Case 2. Crystallization produces a density unstable layer in the upper part of the basic magma sheet, which

continually generates diapirs (inclusions), in accordance with the Rayleigh–Taylor instability theory considered below.

Case 3. Flotation of gas bubbles and their cumulation at the boundary of basic and silicic magmas also cause the Rayleigh–Taylor instability. This may lead to a constant rate of diapir production (Thomas *et al.*, 1993).

INSTABILITY THEORY

The behavior of a density unstable crystallization layer was analyzed in the framework of the Rayleigh–Taylor instability theory (less dense layer under the denser one) (Turner, 1973; Whitehead and Luther, 1975). The instability results in the formation of internal waves in the crystallization layer with a definite distance between the waves. The most rapidly growing waves transform into diapirs rising upward. Distance between diapirs (Y) and the frequency of diapir production (n) are proportional to the thickness of the less dense (buoyant) layer (h) and density difference ($\Delta\rho$), and inversely related to the viscosity of the buoyant layer (μ_3) and viscosity ratio $\alpha = \mu_3/\mu_1$, where μ_1 is the viscosity of the upper sheet. The frequency of diapir production can be taken from the experiments (Whitehead and Luther, 1975):

$$n = (-g\Delta\rho h/4\mu_3)(1 - 0.443\alpha^{4/5}). \quad (1)$$

The distance between the diapir heads (Y) can be related to the thickness of the buoyant layer:

$$2\pi h/Y = 2.5, \quad (2)$$

$$Y \approx 2.5h. \quad (3)$$

As a result, flux of diapirs from the unit area of the layer can be determined. The diapir removal will result in the thinning of the buoyant layer, and from equations (1) - (3) we can determine the downward advance of the upper boundary l_1 with the average velocity V:

$$V = nh(h/Y)^2. \quad (4)$$

Substituting (2) into equation (4), we obtain:

$$V = 0.16nh = 0.16(-g\Delta\rho h^2/4\mu_3)(1 - 0.443\alpha^{4/5}). \quad (5)$$

Now we can see that the velocity of downward propagation of boundary l_1 and the rate of diapir (inclusion) production are determined mainly by the viscosity of the buoyant layer μ_3, the square of the thickness of the layer h, and, to a lesser degree, by the viscosity ratio α.

VISCOSITY OF CRYSTALLIZATION LAYER OF BASIC MAGMA

Viscosity of the three-phase mixture of crystals, gas, and residual melt can be calculated by the approximation of effective viscosity considering the influence of crystals and gas bubbles on the viscosity. The most uncertain parameter in equation (5) is the viscosity of the crystallization layer with a temperature gradient and a related gradient of crystallinity. We used two forms of modeling:

– calculation of the average effective viscosity of the buoyant crystallization layer for each moment in time;

– consideration of the effective viscosity as a free parameter.

Both approaches can be applied to the process under discussion. To calculate the effective viscosity of the buoyant layer, we have to account for the temperature gradient, which causes an increase of the crystallinity degree and the effective magma viscosity from the lower to the upper part of the layer. Following Huppert and Sparks (1988), we assume a linear relationship between inverse temperature (T) and the degree of crystallinity (Xls):

$$Xls = 7200/T - 6, \quad (6)$$

where $1091 < T < 1200$°C.

This equation can be used as the first approximation for the majority of basic igneous rocks, and the effective viscosity can be expressed by the equation (Marsh, 1981):

$$\mu_3 = \mu_2[1 - RXls]^{-2.5}, \quad (7)$$

where R is the parameter of critical crystallinity, equal to 0.67 (Marsh, 1981). This parameter can deviate when critical crystallinity (crystallinity of the closest packing) is higher or lower than 60%, the most frequently used value for magmas. Calculation for each moment in time shows that the temperature gradient through the crystallization layer is approximately linear. This fact was recognized earlier (linear approximation of gradient through hydrodynamic boundary layer) (Richter *et al.*, 1983), and allows us to calculate the effective viscosity μ_3 as an average of viscosities at upper and lower contacts.

The second approximation is justified by the fact that the temperature T_{inv} and degree of crystallinity of density inversion a given magma do not change in time. Hence, the effective viscosity at the lower contact of the buoyant crystallization layer is constant. The temperature of the upper contact of the buoyant crystallization layer may remain constant as well, if diapirs escape from the layer with a certain rate. These conditions define the constant thickness of the crystallization layer for the whole period of crystallization.

NUMERICAL MODEL

Numerical modeling aims to show how the existence of the buoyant crystallization layer, producing diapirs, influences the thermal history of a basic magma sheet and the effectivity of inclusion formation. For simplicity, we performed the modeling in an explicit form for parameters of the most typical basic and silicic magmas (Table 2). Consider our assumptions.

Basic magma may be considered as a flat sheet at the bottom of the silicic magma chamber. Such a struc-

ture could be formed by the replenishment of the chamber with a small portion of basic magma (about 1% of silicic magma volume). Both magmas convect, and basic magma crystallizes both at the contact with silicic magma (in the crystallization layer) and over the whole sheet.

Assume that the whole crystallization layer contains gas bubbles i.e., $T_{sat} = T_{K2}$. In other words, the crystallization front (Marsh, 1989) was intentionally chosen as a front of fluid saturation. Parameters for this case are given in Table 2. For the chosen parameters the basic magma becomes buoyant at 40% of crystallinity.

The temperature profile between boundaries l_1 and l_2 (Fig. 3) is approximated by a polynomial of the second order with free parameters, a, b, and c:

$$T(z) = az^2 + bz + c \quad (8)$$

with gradients at boundaries l_1 and l_2:

$$(\partial T/\partial z)_{l_1} = 2al_1 + b, \quad (9a)$$

$$(\partial T/\partial z)_{l_2} = 2al_2 + b. \quad (9b)$$

Conductive heat fluxes at boundaries l_1 and l_2 are:

$$J_1 = \lambda_1(2al_1 + b), \quad (10a)$$

$$J_2 = \lambda_2(2al_2 + b). \quad (10b)$$

Velocity of downward propagation of the crystallization front (boundary l_2) was estimated using the approach of Worster *et al.*, (1990):

$$k(\partial T/\partial z)_{12} = fq_2(\partial l_1/\partial t) + C2(T_2 - T_{K2})(\partial l_2/\partial t) + F, \quad (11)$$

where F is the convective heat flux from the inner part of a convecting sheet of basic magma:

$$F = 2^{4/3}\lambda_2 k(\beta g/k\mu_2)^{1/3}(T_2 - T_{K2})^{4/3}. \quad (12)$$

The thickness of the dynamic boundary layer (d_1) for the convecting silicic magma was described through the critical Rayleigh number $Ra_C = 1000$, above which, convection occurs (Turner, 1973):

$$d_1 = [1000k\mu_{l_b}/\beta(T_{K1} - T_1)g]^{1/3}, \quad (13)$$

where μ_{l_b} is the average viscosity of this dynamic boundary layer, which can be calculated like μ_3 in equation (7). The thickness of the boundary layer was used for calculating the temperature of the contact T_{K1} assuming a linear relationship between T and z (Richter *et al.*, 1983):

$$T_{K1} = T_1 - d_1(\partial T/\partial z)_{l_1}. \quad (14)$$

For basic magma, a fixed temperature of 25% crystallinity (T_{25}) was accepted as the temperature of the lower contact T_{K2}. The analysis of the crystallization of the convecting magma layer under cooling from above (Worster *et al.*, 1990) shows that the supercooling at the downward propagating boundary l_2 (i.e., $T_{K2} - T_2$) usually does not exceed 1 - 10°C.

The cooling of the interior of the basic magma sheet (T_2) and heating of the silicic magma sheet (T_1) were estimated using a model of effective heat capacities, where the latent heat of crystallization is included into the expression of heat capacity (Sharapov and Cherepanov, 1986):

$$C1ef = C1 + fq_1, \quad (15a)$$

$$C2ef = C2 + fq_2, \quad (15b)$$

where f is defined as $\partial Xls/\partial T$ or the increasing of degree of crystallinity at cooling by 1°C. From the above equations we obtain the rate of temperature change:

$$\partial T_2/\partial t = J_2/C2ef\,LL_2, \quad (16a)$$

$$\partial T_1/\partial t = J_1/C1ef\,LL_1. \quad (16b)$$

Each floating diapir (inclusion) of mass m takes from the basic magma sheet the amount of heat Q equal to the heat of cooling and the latent heat of crystallization of this mass resulting from movement from the isotherm of contact T_{K1} to the isotherm of silicic magma T_1:

$$Q = mC2ef(T_{K1} - T_1). \quad (17)$$

Therefore, the additional heat flux J_3 due to diapir (inclusion) removal from the unit-area of the buoyant and vesiculated crystallization layer for each moment in time can be expressed as:

$$J_2 = VCef(T_{K1} - T_1), \quad (18)$$

where V is the velocity of downward propagation of boundary l_1 (equation(5)).

The equations (10a), (10b), (11), (15a), (15b), and (18) were used in a program to determine the heat balance. They were solved numerically in one dimension z, using the polynomial fitting of the temperature gradient, $T(z)$.

RESULTS: DYNAMICS OF BUOYANT CRYSTALLIZATION LAYER AND GENESIS OF MAFIC INCLUSIONS

The results of calculations show that the thickness of the vesiculated layer of crystallization grows approximately as a square root of time, if diapirs (inclusions) do not form (Fig. 5). This regime is consistent with case 1 (see above). As crystallization proceeds, boundary l_2 moves downward, the thickness of the crystallization layer increases, and temperature gradients and heat fluxes J_1 and J_2 at boundaries l_1 and l_2 decrease. Correspondingly, the isotherms T_{inv} and T_{sat} move downward. The temperature of the interior of the convecting basic magma sheet decreases with time.

For cases 2 and 3 (see above), when the buoyant crystallization layer forms, upper boundary l_1 also moves downward due to the diapir (inclusion) removal with velocity V given in equation (5), and the thickness of the crystallization layer decreases. Thus, the thicken-

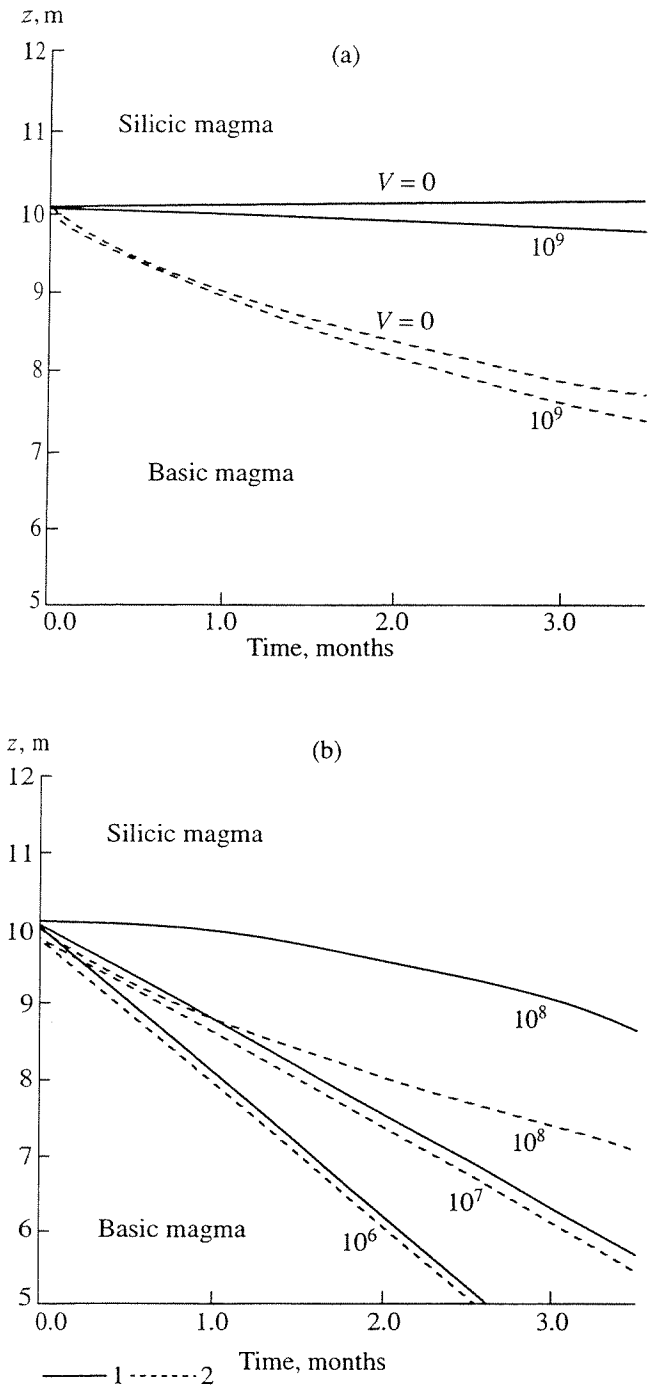

Fig. 5. The dynamics of the upper and lower boundaries of a crystallization layer during crystallization and vesiculation.

(a) diapirs do not remove ($V = 0$) or the rate of removal is small, (b) the rate of diapir removal is high.

Boundaries: 1 – upper l_1, 2 – lower l_2. Values 10^6 - 10^9 indicate different effective viscosities μ_3 (in poise) of the vesiculated layer of crystallization, at which the diapir formation occurs. These viscosities define the initial velocity of vesiculation V in the range from 10^{-4} to 10^{-6} cm/s, respectively. The thickness (z) of the crystallization layer depends mainly on the rate of diapir removal (rate of vesiculation) V.

ing of the crystallization layer as a result of cooling and crystallization is opposed by the thinning caused by the diapir displacement from its upper boundary. Therefore, the dynamics of the crystallization layer depend on the relationship between these two processes or, more specifically, on the relationship between heat fluxes J_1, J_2, F, and J_3. The different regimes of vesiculation discussed above were used for modeling.

Constant vesiculation rate. The mechanism that can cause a relatively constant rate of inclusion formation is related to the cumulation of gas bubbles floating from the interior of the mafic magma sheet to the crystallization layer (case 3). The rate of diapir (inclusion) formation and downward propagation of boundaries l_1 and l_2 will depend on the intensity of the gas bubble flux. This result was confirmed in experiments (Thomas *et al.*, 1993).

For low rates of inclusion formation and gas bubble flux (the velocity of downward propagation of boundary l_1 $V < 5 \times 10^{-5}$ cm/s for the values given in Table 2), J_1 and J_2 exceed J_3; the thickness of the crystallization layer grows as a square root of time, like in the case of $V = 0$ (Fig. 5a).

At a higher velocity of downward propagation of boundary l_1 ($V < 5 \times 10^{-5}$ cm/s), J_3 controls the heat balance. Heat and mass fluxes due to diapir (inclusion) removal govern the thickness of the crystallization layer and make it constant with time. In other words, the velocity of downward propagation of boundary l_1 determines the velocity of propagation of boundary l_2. The higher the rate of diapir formation and removal, the thinner the crystallization layer (Fig. 5). For parameters that are characteristic of the most typical basic and silicic magmas (Table 2), the thickness of the buoyant and vesiculated crystallization layer ranges from a few centimeters to dozens of centimeters (Fig. 5).

Constant viscosity of the buoyant and vesiculated crystallization layer. The approximation of a constant viscosity is valid when J_3 exceeds the fluxes related to the cooling of the basic magma sheet due to diapir removal from the crystallization layer. Under these conditions, the average temperature of the crystallization layer remains constant during the steady-state removal of diapirs. When V is calculated through (5) assuming μ_3 as a free parameter in the range of 10^6 - 10^9 poise, the growth dynamics of the buoyant crystallization layer is strongly dependent on its thickness, h. When h is small (for the initial stages of cooling of the crystallization layer), the rate of vesiculation and diapir formation is small, and the thickness of the crystallization layer increases with time. When increasing h leads to a higher rate V of diapir formation, expressed in equation (5), the process receives its feedback, limiting further growth of the crystallization layer. As a result, we return to the approximation of the constant vesiculation rate considered above.

Lower effective viscosities of the crystallization layer lead to a higher rate of diapir formation and its

thinning. As a consequence, the inclusions are smaller (Fig. 5) and more abundant. For example, if the viscosity of the buoyant and vesiculated crystallization layer is 10^6 - 10^7 poise, the inclusion size of 7 - 20 cm is expected, which is close to the natural observations.

Large and variable viscosity. When the average effective viscosity μ_3 of the buoyant vesiculated crystallization layer exceeds 10^8 poise, and/or its vesiculation rate is small, the dynamics of the crystallization layer can vary. The crystallization layer should thicken with time, as the crystallization rate generally exceeds the rate of diapir formation. The average effective viscosity of the crystallization layer may increase with time, because of the decreasing temperature at its upper contact T_{K1}, which increases the degree of crystallinity and decreases or even terminates the diapir production (see equation (5)). However, the increase of the thickness of the crystallization layer leads to increase (in power of 2) of the inclusion production rate. The net effect depends on the relative values of $\partial\mu_3/\partial t$ and $\partial h/\partial t$.

If the effect of the increase of thickness h on the vesiculation rate is greater than that of the increase in viscosity μ_3, the vesiculation rate becomes constant (Fig. 5b). In this case, according to equation (3), the diapirs will be rather large (dozens of centimeters - few meters) because of the great thickness of the crystallization layer, and the inclusions will be large and few in number. Such inclusions are rare in nature.

If the increase in viscosity dominates, the diapir production stops, and basic magma, less dense than the overlying silicic magma but too viscous to move upward, will crystallize as a porous body under the silicic magma sheet.

Cooling of basic magma in the whole volume and proportions of cumulates and diapirs (inclusions). The cooling of basic magma in its whole volume is directly proportional to the vesiculation rate V: the higher the rate of the inclusion formation the higher the rate of the basic magma cooling (Figs. 5, 6). The latter causes the volume crystallization of the basic magma and cumulate formation at the bottom of the basic magma sheet (Worster *et al.*, 1990).

Figure 7 shows that approximately 50% of the initial volume of basic magma is filled with cumulus crystals, whereas the other half can be removed as diapirs. These crystals can confine up to 50% of the intercumulus melt, and the proportion of cumulates can exceed 75%. Note that the vesiculation and removal of diapirs shorten the time of cooling of the basic magma sheet through an additional heat flux, J_3, related to heat losses by diapir removal; however, the rate of vesiculation does not change the relative proportions of cumulates and diapirs (inclusions).

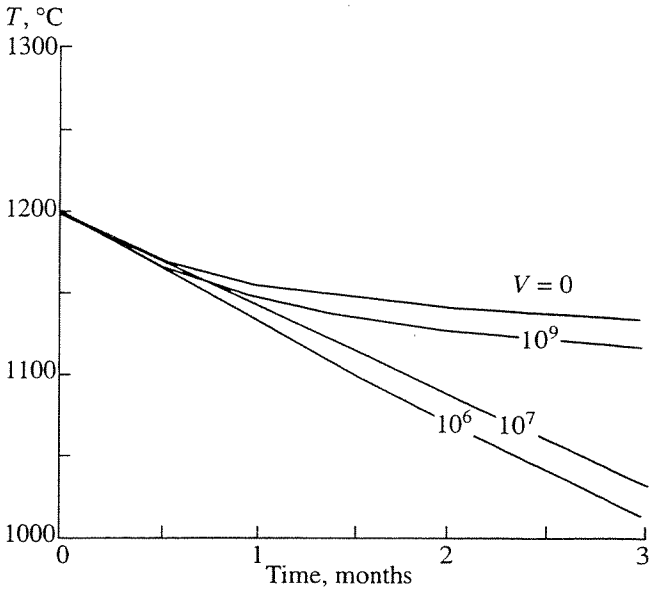

Fig. 6. Volume cooling of basic magma at different rates of diapir (inclusion) removal (Fig. 5, Table 2).

MODEL APPLICATIONS

Observations show that the maximum size of mafic inclusions in volcanic and plutonic rocks rarely exceeds 1 m. According to the instability theory considered above, the size of inclusions is a function of the thickness of the buoyant part of the crystallization layer and is of the same order of magnitude. Growing diapirs (Figs. 1c and 1d) are embryos of mafic inclusions. In contrast to the isothermal experiments (Whitehead and Luther, 1975; Huppert *et al.*, 1982; Thomas *et al.*, 1993), the temperature gradients have to be taken into account. The head of a rising diapir cools and can be rimmed with a chilled margin as it penetrates into the cold silicic magma. As a result, the head of the diapir may become brittle and separate from the diapir tail due to its own buoyancy, or by convection in the interior of the silicic magma sheet. Therefore, the diameter of inclusions is comparable to the diameter of the diapir head and the thickness of the vesiculated layer.

When boundary l_2 moves downward, the temperature of inner parts of the basic magma sheet decreases, and fractionation of basic magma proceeds under the silicic magma sheet. Therefore, the bulk composition of successively formed inclusions becomes more and more evolved. Chemical variations of inclusions in one volcano or even in one lava flow may be explained by this process. However, the differentiation degree of successively removed diapirs is constrained because of the fast accumulation of a cumulate horizon at the bottom of the basic magma sheet. Assuming that convection stops when the proportion of cumulates reaches 50 - 60% (Huppert and Sparks, 1988), we can expect that only 20 - 30% of the sheet can be removed as diapirs through the course of vesiculation (Fig. 7). Meanwhile, the central part of the sheet will be filled with cumulates with or without gas bubbles. Thus, the chem-

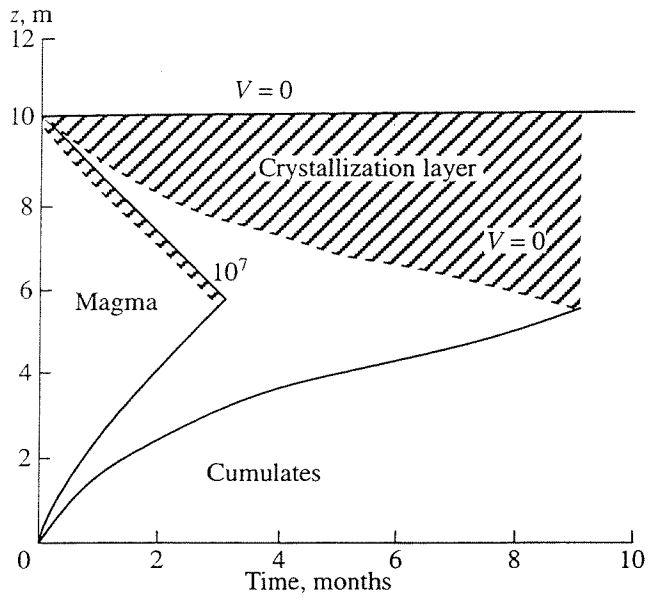

Fig. 7. The thickness (z) decrease of basic magma sheet due to diapir (inclusion) removal and cumulate formation at the bottom of the chamber (Fig. 5, Table 2).

ical evolution of inclusions which should be restricted to 20 - 30% of differentiation of the initial basaltic magma, i.e., inclusions which are capable of reaching the composition of basaltic andesites or andesites. This is consistent with the compositions of natural mafic inclusions.

The layer of mafic cumulates formed at the bottom of the chamber can be mixed with silicic magma over the whole volume of the silicic magma chamber by convection. Porous and buoyant mafic inclusions can float up and concentrate at the upper parts of the silicic chamber or in conduits (Bindeman, 1993), and can be easily erupted during volcanic events. Flotation of mafic inclusions with gas bubbles can strongly increase the internal pressure in the magma chamber through the mechanism of gas lifting (Bindeman and Podladchikov, 1991).

CONCLUSION

The proposed model is not the only possible model to explain the genesis of mafic inclusions and mixing of compositionally contrasting magmas. The goal of the paper is to attract attention to the vesiculation of basic magma and its effect on the mixing of contrasting magmas, particularly in shallow-level chambers and intrusions, where the effect of density decreasing should be the most pronounced.

ACKNOWLEDGMENTS

The author is grateful to Fred Anderson, Steve Wickham (University of Chicago), George Berngantz (University of Washington), Yurii Podladchikov (Vrije University, Amsterdam), and N.N. Bindeman (ZNIGRI MinGeo, Moscow) for careful reviews and fruitful discussion, and Yu.S. Genshaft (Institute of Earth's Physics, Moscow) for the support of this work.

REFERENCES

Anderson, A.T., Magma Mixing: Petrological Process and Volcanological Tool, *J. Volcanol. Geotherm. Res.*, 1976, no. 1, pp. 3 - 33.

Bacon, C.R., Magmatic Inclusions in Silicic and Intermediate Rocks, *J. Geophys. Res.*, 1986, vol. B 91, no. 6, pp. 6091 - 6112.

Barbarin, B., Enclaves of the Mesozoic Calc-Alkaline Granitoids of the Sierra Nevada Batholith, *Devel. Petrol.: Enclaves and Granite Petrology*, Barbarin, B. and Didier, J., Eds., 1991, vol. 13, pp. 135 - 153.

Bindeman, I.N., A Practical Petrological Method for Determination of Volume Proportions of Magma Chamber Refilling, *J. Volcanol. Geotherm. Res.*, 1993, vol. 56, pp. 133 - 144.

Bindeman, I.N., Petrological and Experimental Models of the Mixing of Contrasting Silicate Magmas, *Cand. Sci. (Geol). Dissertation*, Moscow State University, 1991, 27 p.

Bindeman, I.N. and Bailey, J.C., A Model of Reverse Differentiation on Dikii Greben' Volcano (Kamchatka): Progressive Mafic Magma Vesiculation in a Magma Chamber, *Contrib. Mineral. Petrol.*, 1994, vol. 117, pp. 263 - 278.

Bindeman, I.N. and Podladchikov, Yu.Yu., On the Mechanism of Transport and Eruption of Cognate Inclusions in Igneous Rocks, *Izv. Akad. Nauk SSSR., Ser. Geol.*, 1991, no. 4, pp. 48 - 56.

Burnham, C.W., Holloway, J.R., and Davis, N.F., Thermodynamic Properties of Water to 1000°C and 10 000 Bars, *Geol. Soc. Am., Spec. Pap.*, 1969, p. 132.

Campbell, I.H. and Turner, J.S., Fountains in Magma Chambers, *J. Petrol.*, 1989, vol. 30, pp. 885 - 923.

Campbell, I.H. and Turner, J.S., Turbulent Mixing of Fluids with Different Viscosities, *Nature*, 1985, vol. 313, pp. 613 - 616.

Eichelberger, J.C., Vesiculation of Mafic Magma during Replenishment of Silicic Magma Reservoirs, *Nature*, 1980, vol. 288, pp. 446 - 451.

Eggler, D.H., Amphibole Stability in H_2O Undersaturated Calc-Alkaline Melt, *Earth Planet. Sci. Lett.*, 1973, vol. 15, pp. 28 - 34.

Freundt, A. and Schmincke, H.-U., Mixing of Rhyolite, Trachyte and Basalt Magma Erupted from a Vertical and Laterally Zoned Reservoir, Composite Flow P1, Gran Canaria, *Contrib. Mineral. Petrol.*, 1992, vol. 112, pp. 1 - 19.

Frolova, T.I., Bindeman, I.N., Mostafa, M., and Bailey J.C., Mafic Inclusions in Andesites and Dacites from the Volcanoes of the Kamchatka and Kuriles, *Izv. Ross. Akad. Nauk, Ser. Geol.*, 1992, no. 4, pp. 52 - 63.

Huppert, H.E. and Sparks, R.S.J., The Generation of Granitic Magmas, *J. Petrol.*, 1988, vol. 29, pp. 599 - 624.

Huppert, H.E., Sparks, R.S.J., and Turner, J.S., Effect of Volatiles on Mixing in Calc-Alkaline Magma System, *Nature*, 1982, vol. 297, pp. 554 - 557.

Kadik, A.A., Lukanin, O.A., Lebedev, E.B., and Korovushkina, E.E., Water and Carbon Dioxide Solubility in Granitic and Basaltic Magmas at High Pressure, *Geokhimiya*, 1973, no. 9, pp. 1041 - 1050.

Kadik, A.A., Maksimov, A.P., and Ivanov, B.V., *Fisiko-Khimicheskie Usloviya Kristallizatsii i Genezis Andezitov* (Physico-Chemical Conditions of Crystallization and Genesis of Andesites), Moscow: Nauka, 1986.

Koyaguchi, T., Enclaves from Volcanic Rocks from Japan, *Development in Petrology: Enclaves and Granite Petrology*, Barbarin, B. and Didier, J., Eds., 1991, vol. 13, pp. 187 - 198.

Litvinovskii, B.A., Zanzilevich, A.N., Kalmanovich, M.A., and Shadaev, M.M., Synplutonic Basic Intrusions of Early Stages of Emplacement of the Angaro-Vitim Batholith (Zabaikal'e), *Geol. Geofiz.*, 1992, no. 7, pp. 70 - 81.

Marsh, B.D., On Convective Style and Vigor in Sheet-Like Magma Chambers, *J. Petrol.*, 1989, vol. 30, pp. 479 - 530.

Marsh, B.D., On Crystallinity, Probability of Occurrence, and Rheology of Lava and Magma, *Contrib. Mineral. Petrol.*, 1981, vol. 78, no. 1, pp. 85 - 98.

Richter, F.M., Nataf, H.-C., and Daly, S.F., Heat Transfer and Horizontally Averaged Temperature of Convection with Large Viscosity Variations, *J. Fluid Mech.*, 1983, vol. 129, pp. 173 - 192.

Sharapov, V.N. and Cherepanov, A.N., *Dinamika Differentsiatsii Magm* (Dynamics of Magma Differentiation), Novosibirsk: Nauka, 1985.

Shilobreeva, S.I. and Kadik, A.A., CO_2 Solubility in Basic and Silicic Magmas, *Tezisy 2-i Konf. "Magma i Magmaticheskie Fluidy,"* (Abstr. of the 2nd Conference Magma and Magmatic Fluids), Chernogolovka, 1985, pp. 201 - 204.

Shmonov, V.M. and Shmulovich, K.I., Specific Volumes and Equations of State of Carbon Dioxide at Temperatures of 100 - 1000°C and Pressures 2 - 10 000 bar, *Dokl. Akad. Nauk SSSR*, 1978, vol. 217, no. 2, pp. 206 - 209.

Sparks, R.S.J., Sigurdsson, H., and Wilson, L., Magma Mixing: Mechanism for Triggering Acid Explosive Eruptions, *Nature*, 1977, vol. 257, pp. 315 - 318.

Thomas, N., Tait, S., and Koyaguchi, T., Mixing of Stratified Liquids by Motion of Gas Bubbles: Application to Magma Mixing, *Earth Planet. Sci. Lett.*, 1993, vol. 15, pp. 161 - 175.

Turner, J.S., *Buoyancy Effect in Fluid*, Cambridge Univ. Press, 1973.

Turner, J.S. and Campbell, I.H., Convection and Mixing in Magma Chambers, *Earth Sci. Rev.*, 1986, vol. 23, no. 4, pp. 255 - 352.

Wiebe, R., Basaltic Injections into Floored Silicic Magma Chambers, *EOS Trans.*, 1993, vol. 74 (1), pp. 1 - 3.

Whitehead, J.A., Jr. and Luther, D.S., Dynamics of Laboratory Diapirs and Plumes, *J. Geophys. Res.*, 1975, vol. 80, pp. 705 - 717.

Worster, M.G., Huppert, H.E., and Sparks, R.S.J., Convection and Crystallization in Magma Cooled from Above, *Earth Planet. Sci. Lett.*, 1990, vol. 101, pp. 78 - 89.

Zlobin, T.K., *Glubinnaya Struktura i Geodinamika Kuril'skoi Ostrovnoi Dugi* (Deep Structure and Geodynamics of the Kurile Island Arc), Yuzhno-Sakhalinsk: Dal'nevostochnoe Knizhnoe Izdatel'stvo, 1989.